arXiv:1605.06059v1 [hep-ph] 19 May 2016

THE $b \to s\ell^+\ell^-$ ANOMALIES AND THEIR IMPLICATIONS FOR NEW PHYSICS

S. DESCOTES-GENON
Laboratoire de Physique Théorique, CNRS/Univ. Paris-Sud 11 (UMR 8627)
91405 Orsay Cedex, France

L. HOFER [a]
Department de Física Quàntica i Astrofísica (FQA)
Institut de Ciències del Cosmos (ICCUB)
Universitat de Barcelona (UB), Martí Franquès 1
08028 Barcelona, Spain

J. MATIAS
Universitat Autònoma de Barcelona
08193 Bellaterra, Spain

J. VIRTO
Theoretische Physik 1, Naturwissenschaftlich-Technische Fakultät
Universität Siegen, 57068 Siegen, Germany

Recently, the LHC has found several anomalies in exclusive semileptonic $b \to s\ell^+\ell^-$ decays. In this proceeding, we summarize the most important results of our global analysis of the relevant decay modes. After a discussion of the hadronic uncertainties entering the theoretical predictions, we present an interpretation of the data in terms of generic new physics scenarios. To this end, we have performed model-independent fits of the corresponding Wilson coefficients to the data and have found that in certain scenarios the best fit point is prefererred over the Standard Model by a global significance of more than 4σ. Based on the results, the discrimination between high-scale new physics and low-energy QCD effects as well as the possibility of lepton-flavour universality violation are discussed.

1 Introduction

The flavour-changing neutral current (FCNC) transition $b \to s\ell^+\ell^-$ can be probed through various decay channels, currently studied in detail at the LHC in the LHCb, CMS and ATLAS experiments, as well as at Belle. Recent experimental results have shown interesting deviations from the SM: The LHCb analysis [1] of the $3\,\text{fb}^{-1}$ data on $B \to K^*\mu^+\mu^-$ in particular confirms a $\sim 3\sigma$ anomaly in two large K^*-recoil bins of the angular observable P_5' [2,3] that was already present in the $1\,\text{fb}^{-1}$ results presented in 2013 [4]. The observable $R_K = Br(B \to K\mu^+\mu^-)/Br(B \to Ke^+e^-)$ was measured by LHCb [5] in the dilepton mass range from 1 to 6 GeV^2 as $0.745^{+0.090}_{-0.074} \pm 0.036$, corresponding to a 2.6σ tension with its SM value predicted to be equal to 1 (to a very good accuracy). Finally, also the LHCb results [6] on the branching ratio of $B_s \to \phi\mu^+\mu^-$ exhibit deviations at the $\sim 3\sigma$ level in two large-recoil bins.

[a] talk given by L. Hofer at the 51st Rencontres de Moriond EW 2016

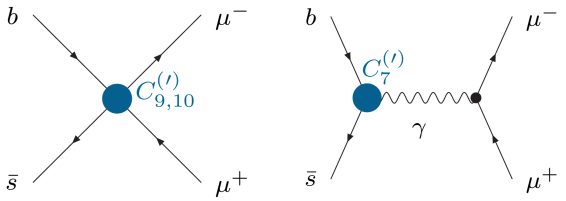

processes	$\mathcal{C}_7^{(\prime)}$	$\mathcal{C}_9^{(\prime)}$	$\mathcal{C}_{10}^{(\prime)}$
$B \to X_s\gamma$, $B \to K^*\gamma$	✓		
$B \to X_s\mu^+\mu^-$	✓	✓	✓
$B_s \to \mu^+\mu^-$			✓
$B_{(s)} \to (K^{(*)}, \phi)\mu^+\mu^-$	✓	✓	✓

Figure 1 – Effective couplings $\mathcal{C}_{7,9,10}^{(\prime)}$ contributing to $b \to s\ell^+\ell^-$ transitions and sensitivity of the various radiative and (semi-)leptonic $B_{(s)}$ decays to them.

The appearance of several tensions in different $b \to s\ell^+\ell^-$ channels is quite intriguing because all these observables are sensitive to the same effective couplings $\mathcal{C}_{7,9,10}^{(\prime)}$ illustrated in Fig. 1 and induced by the operators

$$\mathcal{O}_9^{(\prime)} = \frac{\alpha}{4\pi}[\bar{s}\gamma^\mu P_{L(R)}b][\bar{\mu}\gamma_\mu\mu], \qquad \mathcal{O}_{10}^{(\prime)} = \frac{\alpha}{4\pi}[\bar{s}\gamma^\mu P_{L(R)}b][\bar{\mu}\gamma_\mu\gamma_5\mu],$$
$$\mathcal{O}_7^{(\prime)} = \frac{\alpha}{4\pi}m_b[\bar{s}\sigma_{\mu\nu}P_{R(L)}b]F^{\mu\nu}, \tag{1}$$

where $P_{L,R} = (1 \mp \gamma_5)/2$ and m_b denotes the b quark mass. It is thus natural to ask whether a new physics contribution to these couplings could simultaneously account for the various tensions in the data. Beyond the SM, contributions to $\mathcal{C}_{9,10}^{(\prime)}$ are for instance generated at tree level in scenarios with Z' bosons or lepto–quarks. Note that additional scalar or pseudoscalar couplings $\mathcal{C}_{S,S',P,P'}$ cannot address the above-mentioned anomalies since their contributions are suppressed by small lepton masses. Therefore we will not discuss this possibility in the following.

The parameter space spanned by the couplings $\mathcal{C}_{7,9,10}^{(\prime)}$ is probed through various observables in radiative and (semi-)leptonic $B_{(s)}$ decays, each of them sensitive to a different subset of coefficients (see Fig. 1). A complete investigation of potential new physics effects thus requires a combined study of these observables including correlations among them. The first analysis in this spirit, performed in Ref. [7] with the data of 2013, pointed to a large negative contribution to the Wilson coefficient $\mathcal{C}_9$. This general picture was confirmed later on by other groups, using different/additional observables, different theoretical input for the form factors etc. (e.g. Refs. [8,9]). In this proceeding, we report the most important results of our analysis in Ref. [10] which can be compared to other recent global analyses [11,12,13] and which improves the original study in Ref. [7] in many aspects: It includes the latest experimental results of all relevant decays (using the LHCb data for the exclusive), uses refined techniques to estimate uncertainties originating from power corrections to the hadronic form factors and from non-perturbative charm loops, and consistently takes into account experimental and theoretical correlations.

Before presenting the results from our fits in Sec. 3, with a special emphasis on the possibility of discriminating between high-scale new physics and low-energy QCD effects as well as on the possibility of lepton-flavour universality violation, we discuss in Sec. 2 the hadronic uncertainties entering the theoretical predictions of the relevant observables. Our conclusions are given in Sec. 4.

2 Hadronic uncertainties

Predictions for exclusive semileptonic B decays are plagued by QCD effects of perturbative and non-perturbative nature. At leading order (LO) in the effective theory, predictions involve tree-level diagrams with insertions of the operators $\mathcal{O}_{7,9,10}$ (generated at one loop in the SM), as well as one-loop diagrams with an insertion of the charged-current operator $\mathcal{O}_2 = [\bar{s}\gamma^\mu P_L c][\bar{c}\gamma_\mu P_L b]$ (generated at tree level in the SM). In contributions of the first type, the leptonic and the hadronic currents factorize, and QCD corrections are constrained to the hadronic $B \to M$ current (first two diagrams in Fig. 2). This class of *factorizable QCD corrections* thus forms

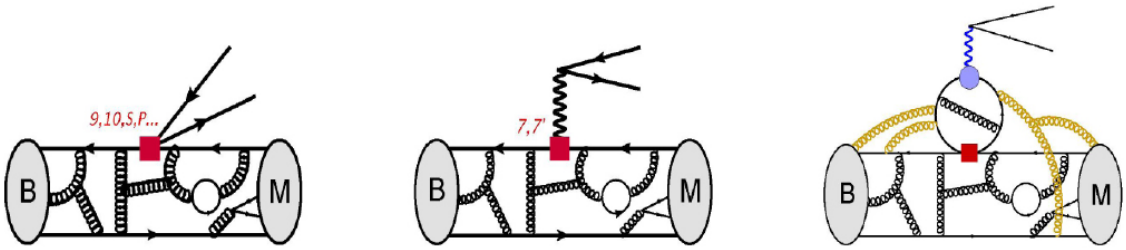

Figure 2 – Illustration of factorizable (first two diagrams) and non-factorizable (third diagram) QCD corrections to exclusive $B \to M\ell^+\ell^-$ matrix elements.

part of the hadronic form factors parametrizing the $B \to M$ transition. Contributions of the second type, on the other hand, receive *non-factorizable QCD corrections* (third diagram in Fig. 2) that cannot be absorbed into form factors. In the following we discuss the uncertainties stemming from the two types of corrections and their implementation in our analysis.

2.1 Form factor uncertainties

The form factors are available from lattice as well as from light-cone sum rule (LCSR) calculations, with the former being suited for the region of high $q^2 > 15\,\text{GeV}^2$ and the latter for the region of low $q^2 < 8\,\text{GeV}^2$. Since the form factors introduce a dominant source of uncertainties into the theory predictions, it is desirable to reduce the sensitivity to them as much as possible. For $B \to V\ell^+\ell^-$ decays, with V being a vector meson, this can be achieved in the low-q^2 region by exploiting large-recoil symmetries of QCD. At LO in α_s and Λ/m_b, these symmetries enforce certain relations among the seven hadronic form factors V, A_1, A_2, A_0, T_1, T_2, T_3, like e.g.

$$\frac{m_B(m_B + m_{K^*})A_1 - 2E(m_B - m_{K^*})A_2}{m_B^2 T_2 - 2Em_B T_3} = 1 + \mathcal{O}(\alpha_s, \Lambda/m_b), \tag{2}$$

where m_B denotes the mass of the B meson, and m_{K^*} and E the mass and the energy of the K^* meson. From the experimentally measured coefficients of the differential angular distribution of $B \to V\ell^+\ell^-$, one can construct observables that involve ratios like the one in eq. (2). The resulting observables $P_i^{(\prime)}$ then only exhibit a mild form factor dependence, suppressed by powers of α_s and Λ/m_b.

For the cancellation of the form factor uncertainties in ratios like the one in eq. (2), it is crucial to have control of the correlations among the errors of the different form factors. These correlations can be taken into account via two orthogonal approaches: Either they can be assessed directly from the LCSR calculation (Ref. [14] provides LCSR form factors with correlation matrices), or they can be implemented resorting to the large-recoil symmetry relations. Whereas the former method is limited to the particular set of LCSR form factors from Ref. [14] and hence sensitive to details of the corresponding calculation, the latter method determines the correlations in a model-independent way from first principles and can thus also be applied to different sets of form factors like the ones from Ref. [15], where no correlations were provided. As a drawback, correlations are obtained from large-recoil symmetries only up to Λ/m_b corrections which have to be estimated. For the estimate of these *factorizable power corrections*, we follow the strategy that was developed in Ref. [16] based on and further refining a method first proposed in Ref. [17]. We assume a generic size of 10% factorizable power corrections to the form factors, which is consistent with the results that are obtained from a fit to the particular LCSR form factors from Refs. [15,14].

Coefficient	Best fit	1σ	3σ	Pull_{SM}
$\mathcal{C}_7^{\text{NP}}$	-0.02	$[-0.04, -0.00]$	$[-0.07, 0.03]$	1.2
$\boldsymbol{\mathcal{C}_9^{\text{NP}}}$	$\mathbf{-1.09}$	$[-1.29, -0.87]$	$[-1.67, -0.39]$	**4.5**
$\mathcal{C}_{10}^{\text{NP}}$	0.56	$[0.32, 0.81]$	$[-0.12, 1.36]$	2.5
$\mathcal{C}_{7'}^{\text{NP}}$	0.02	$[-0.01, 0.04]$	$[-0.06, 0.09]$	0.6
$\mathcal{C}_{9'}^{\text{NP}}$	0.46	$[0.18, 0.74]$	$[-0.36, 1.31]$	1.7
$\mathcal{C}_{10'}^{\text{NP}}$	-0.25	$[-0.44, -0.06]$	$[-0.82, 0.31]$	1.3
$\mathcal{C}_9^{\text{NP}} = \mathcal{C}_{10}^{\text{NP}}$	-0.22	$[-0.40, -0.02]$	$[-0.74, 0.50]$	1.1
$\boldsymbol{\mathcal{C}_9^{\text{NP}} = -\mathcal{C}_{10}^{\text{NP}}}$	$\mathbf{-0.68}$	$[-0.85, -0.50]$	$[-1.22, -0.18]$	**4.2**
$\boldsymbol{\mathcal{C}_9^{\text{NP}} = -\mathcal{C}_{9'}^{\text{NP}}}$	$\mathbf{-1.06}$	$[-1.25, -0.85]$	$[-1.60, -0.40]$	**4.8**

Table 1: Results of various one-parameter fits for the Wilson coefficients $\{\mathcal{C}_i\}$.

2.2 Uncertainties from $c\bar{c}$ loops

Long-distance charm-loop effects (third diagram in Fig. 2) can mimic the effect of an effective coupling $\mathcal{C}_9^{c\bar{c}}$ and have been suggested as a solution of the anomaly in $B \to K^* \mu^+ \mu^-$ [20,21]. Due to the non-local structure of these corrections, their contribution is expected to have a non-constant q^2-dependence, where q^2 is the squared invariant masses of the lepton pair. Together with the perturbative SM contribution $\mathcal{C}_{9\,\text{SM pert}}^{\text{eff}}$ and a potential constant new physics coupling $\mathcal{C}_9^{\text{SM}}$, it can be cast into an effective Wilson coefficient

$$\mathcal{C}_9^{\text{eff i}}(q^2) = \mathcal{C}_{9\,\text{SM pert.}}^{\text{eff}}(q^2) + \mathcal{C}_9^{\text{NP}} + \mathcal{C}_9^{c\bar{c}\,i}(q^2), \tag{3}$$

with a different $\mathcal{C}_9^{c\bar{c}\,i}$ and hence also a different $\mathcal{C}_9^{\text{eff i}}$ for the three transversity amplitudes $i = 0, \|, \perp$. Currently, only a partial calculation [15] exists, yielding values $\mathcal{C}_{9\,\text{KMPW}}^{c\bar{c}\,i}$ that tend to enhance the anomalies. In our analysis, we assume that this partial result is representative for the order of magnitude of the total charm-loop contribution and we assign an error to unknown charm-loop effects varying

$$\mathcal{C}_9^{c\bar{c}\,i}(q^2) = s_i\, \mathcal{C}_{9\,\text{KMPW}}^{c\bar{c}\,i}(q^2), \quad \text{for } -1 \le s_i \le 1. \tag{4}$$

3 Results of the global fit

Our reference fits are obtained using the following experimental input: branching ratios and angular observables of the decays $B \to K^* \mu^+ \mu^-$ and $B_s \to \phi \mu^+ \mu^-$, branching ratios of the charged and neutral modes $B \to K \mu^+ \mu^-$, the branching ratios of $B \to X_s \mu^+ \mu^-$, $B_s \to \mu^+ \mu^-$ and $B \to X_s \gamma$, as well as the isospin asymmetry A_I and the time-dependent CP asymmetry $S_{K^*\gamma}$ of $B \to K^* \gamma$. For the theoretical predictions, we use lattice form factors from Refs. [18,19] in the low-recoil region, and LCSR form factors from Ref. [15] (except for $B_s \to \phi$ where Ref. [14] is used), with correlations assessed from the large-recoil symmetries.

Starting from a model hypothesis with n free parameters for the Wilson coefficients $\{\mathcal{C}_i^{\text{NP}}\}$, we then perform a frequentist $\Delta\chi^2$-fit, including experimental and theoretical correlation matrices. In Tab. 1 we show our results for various one-parameter scenarios. In the last column we give the SM-pull for each scenario, i.e. we quantify by how many sigmas the best fit point is preferred over the SM point $\{\mathcal{C}_i^{\text{NP}}\} = 0$ in the given scenario. A scenario with a large SM-pull thus allows for a big improvement over the SM and a better description of the data. From the results in Tab. 1 we infer that a large negative $\mathcal{C}_9^{\text{NP}}$ is required to explain the data. In a scenario

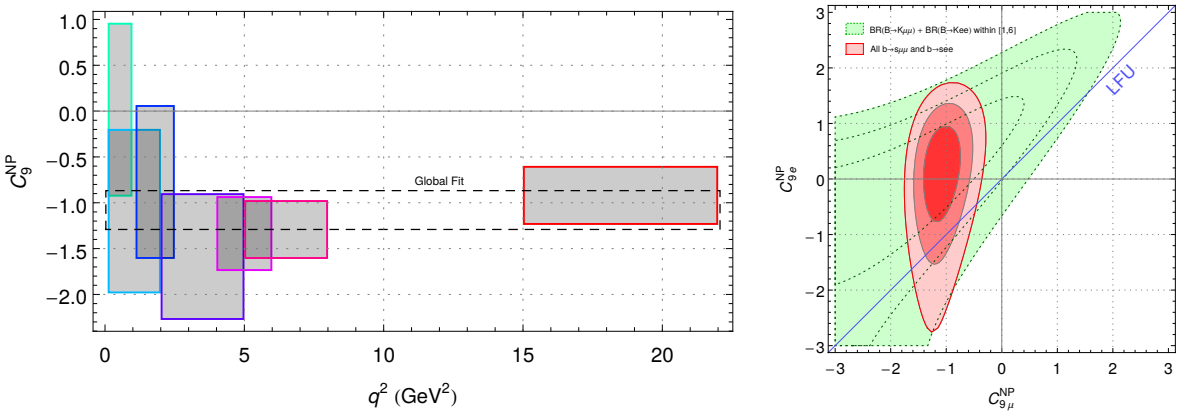

Figure 3 – Left: Bin-by-bin fit of the one-parameter scenario with a single coefficient $\mathcal{C}_9^{\rm NP}$. Right: Fit with independent coefficients $\mathcal{C}_{9\,\mu}^{\rm NP}$ and $\mathcal{C}_{9\,e}^{\rm NP}$.

where only this coefficient is generated a fairly good goodness-of-fit is yielded for $\mathcal{C}_9^{\rm NP} \sim -1.1$. A decomposition into the different exclusive decay channels, as well as into low- and large-recoil regions, shows that each of these individual contributions points to the same solution, i.e. a negative $\mathcal{C}_9^{\rm NP}$, albeit with varying significance. We refer the reader to Ref. [10] for further results, e.g. for fits in various 2-parameter scenarios as well as for the full 6-parameter fit of $\mathcal{C}_{7,9,10}^{(\prime)\rm NP}$ resulting in a SM-pull of 3.6σ.

3.1 New physics vs. non-perturbative charm-contribution

According to Eq. (3), a potential new physics contribution $\mathcal{C}_9^{\rm NP}$ enters amplitudes always together with a charm-loop contribution $\mathcal{C}_9^{c\bar{c}\,i}(q^2)$, spoiling an unambiguous interpretation of the fit result from the previous section in terms of new physics. However, whereas $\mathcal{C}_9^{\rm NP}$ does not depend on the squared invariant mass q^2 of the lepton pair, $\mathcal{C}_9^{c\bar{c}\,i}(q^2)$ is expected to exhibit a non-trivial q^2-dependence. Following Ref. [12], we show in Fig. 3 on the left a bin-by-bin fit for the one-parameter scenario with a single coefficient $\mathcal{C}_9^{\rm NP}$. The results obtained in the individual bins are consistent with each other, allowing thus for a solution $\mathcal{C}_9^{\rm NP}$ that is constant in the whole q^2 region, as required for an interpretation in terms of new physics, though the situation is not conclusive due to the large uncertainties in the single bins.

An alternative strategy to address this question has been followed recently in Ref. [21] where a direct fit of the q^2-dependent charm contribution $\mathcal{C}_9^{c\bar{c}\,i}(q^2)$ to the data on $B \to K^*\mu^+\mu^-$ (at low q^2) has been performed under the hypothesis of the absence of new physics. The fact that only one out of the 12 parameters encoding a non-constant q^2-dependence in $\mathcal{C}_9^{c\bar{c}\,i}(q^2)$ differs from zero by $\gtrsim 2\sigma$ makes the result obtained in Ref. [21] compatible [b] with a q^2-independent new physics solution $\mathcal{C}_9^{\rm NP}$, in agreement with our findings from Fig. 3. Note further that the results in Ref. [21] do not allow to draw any conclusions on whether a q^2-dependent solution of the anomalies via $\mathcal{C}_9^{c\bar{c}\,i}(q^2)$ is preferred compared to a solution via a constant $\mathcal{C}_9^{\rm NP}$ since this would require a comparison of the goodness of the fit taking into account the different number of free parameters of the two parametrizations. Moreover, we like to stress that the results for the observables presented in Ref. [21] should not be interpreted as SM predictions, as they are based on a fit to the experimental data.

[b] The probability for a fluctuation by $\gtrsim 2\sigma$ in at least one out of 12 parameters is given by $1 - 0.954^{12} \approx 43\%$, well within 1σ.

3.2 Lepton-flavour universality violation

Since the measurement of R_K suggests the violation of lepton-flavour universality, we also studied the situation where the muon- and the electron-components of the operators $\mathcal{C}^{(\prime)}_{9,10}$ receive independent new physics contributions $\mathcal{C}^{\rm NP}_{i\,\mu}$ and $\mathcal{C}^{\rm NP}_{i\,e}$, respectively. The electron-couplings $\mathcal{C}^{\rm NP}_{i\,e}$ are constrained by adding the decays $B \to K^{(*)}e^+e^-$ to the global fit. Note that the correlated fit to $B \to K\mu^+\mu^-$ and $B \to Ke^+e^-$ simultaneously is equivalent to a direct inclusion of the observable R_K.

In Fig. 3 on the right we display the result for the two-parameter fit to the coefficients $\mathcal{C}^{\rm NP}_{9\,\mu}$ and $\mathcal{C}^{\rm NP}_{9\,e}$. The fit prefers an electron-phobic scenario with new physics coupling to $\mu^+\mu^-$ but not to e^+e^-. Under this hypothesis, that should be tested by measuring R_{K^*} and R_ϕ, the SM-pull increases by $\sim 0.5\sigma$ compared to the value in Tab. 1 for the lepton-flavour universal scenario.

4 Conclusions

LHCb data on $b \to s\ell^+\ell^-$ decays shows several tensions with SM predictions, in particular in the angular observable P_5' of $B \to K^*\mu^+\mu^-$, in the branching ratio of $B_s \to \phi\mu^+\mu^-$, and in the ratio $R_K = Br(B \to K\mu^+\mu^-)/Br(B \to Ke^+e^-)$ (all of them at the $\sim 3\sigma$ level). In global fits of the Wilson coefficients to the data, scenarios with a large negative $\mathcal{C}^{\rm NP}_9$ are preferred over the SM by typically more than 4σ. A bin-by-bin analysis demonstrates that the fit is compatible with a q^2-indepedent effect generated by high-scale new physics, though a q^2-dependent QCD effect cannot be excluded with the current precision. Note, however, that a QCD effect could not explain the tension in R_K. The latter observable further favours a lepton-flavour violating scenario with new physics coupling only to $\mu^+\mu^-$ but not to e^+e^-, a scenario to be probed by a measurement of the analogous ratios R_{K^*} and R_ϕ to probe this hypothesis.

Acknowledgments

L.H. is grateful to the organizers for the invitation to the workshop and thanks the participants for stimulating discussions. The work of L.H. was supported by the grants FPA2013-46570-C2-1-P and 2014-SGR-104, and partially by the Spanish MINECO under the project MDM-2014-0369 of ICCUB (Unidad de Excelencia "María de Maeztu"). JV is funded by the DFG within research unit FOR 1873 (QFET), and acknowledges financial support from CNRS. SDG, JM and JV acknowledge financial support from FPA2014-61478-EXP. This project has received funding from the European Unions Horizon 2020 research and innovation programme under grant agreements No 690575, No 674896 and No. 692194.

References

1. R. Aaij *et al.* [LHCb Collaboration], arXiv:1512.04442 [hep-ex].
2. S. Descotes-Genon, J. Matias, M. Ramon and J. Virto, JHEP **1301** (2013) 048, arXiv:1207.2753 [hep-ph].
3. S. Descotes-Genon, T. Hurth, J. Matias and J. Virto, JHEP **1305** (2013) 137, arXiv:1303.5794 [hep-ph].
4. **LHCb** Collaboration, PRL **111** (2013) 191801, arXiv:1308.1707 [hep-ex].
5. **LHCb** Collaboration, Phys. Rev. Lett. **113** (2014) 151601, arXiv:1406.6482 [hep-ex].
6. **LHCb** Collaboration, JHEP **1307** (2013) 084, arXiv:1305.2168 [hep-ex].
7. S. Descotes-Genon, J. Matias and J. Virto, Phys. Rev. D **88** (2013) 074002, arXiv:1307.5683 [hep-ph].
8. W. Altmannshofer and D. M. Straub, Eur. Phys. J. C **73** (2013) 2646 arXiv:1308.1501 [hep-ph].

9. F. Beaujean, C. Bobeth and D. van Dyk, Eur. Phys. J. C **74** (2014) 2897 [Eur. Phys. J. C **74** (2014) 3179], arXiv:1310.2478 [hep-ph].
10. S. Descotes-Genon, L. Hofer, J. Matias and J. Virto, arXiv:1510.04239 [hep-ph].
11. W. Altmannshofer and D. M. Straub, Eur. Phys. J. C **75** (2015) 8, 382, arXiv:1411.3161 [hep-ph].
12. W. Altmannshofer and D. M. Straub, arXiv:1503.06199 [hep-ph].
13. T. Hurth, F. Mahmoudi and S. Neshatpour, arXiv:1603.00865 [hep-ph].
14. A. Bharucha, D. M. Straub and R. Zwicky, arXiv:1503.05534 [hep-ph].
15. A. Khodjamirian, T. Mannel, A. A. Pivovarov and Y.-M. Wang, JHEP **1009** (2010) 089, arXiv:1006.4945 [hep-ph].
16. S. Descotes-Genon, L. Hofer, J. Matias and J. Virto, JHEP **1412** (2014) 125, arXiv:1407.8526 [hep-ph].
17. S. Jäger and J. Martin Camalich, JHEP **1305** (2013) 043, arXiv:1212.2263 [hep-ph].
18. R. R. Horgan, Z. Liu, S. Meinel and M. Wingate, Phys. Rev. D **89** (2014) 9, 094501, arXiv:1310.3722 [hep-lat], PoS LATTICE **2014** (2015) 372, arXiv:1501.00367 [hep-lat].
19. C. Bouchard *et al.* [HPQCD Collaboration], Phys. Rev. D **88** (2013) 5, 054509 [Phys. Rev. D **88** (2013) 7, 079901], arXiv:1306.2384 [hep-lat].
20. J. Lyon and R. Zwicky, arXiv:1406.0566 [hep-ph].
21. M. Ciuchini *et al.* , arXiv:1512.07157 [hep-ph].